



# Extinction Coefficients retrieved in Deep Tropical Ice Clouds from Lidar Observations using a CALIPSO-like Algorithm compared to In-Situ Measurements from the Cloud Integrating Nephelometer during CRYSTAL-FACE

Vincent Noel, David M. Winker, Tim J. Garrett, Matthew M. McGill

## ► To cite this version:

Vincent Noel, David M. Winker, Tim J. Garrett, Matthew M. McGill. Extinction Coefficients retrieved in Deep Tropical Ice Clouds from Lidar Observations using a CALIPSO-like Algorithm compared to In-Situ Measurements from the Cloud Integrating Nephelometer during CRYSTAL-FACE. *Atmospheric Chemistry and Physics*, 2007, 7, pp.1-8. halsde-00136133

**HAL Id: halsde-00136133**

**<https://hal.science/halsde-00136133>**

Submitted on 12 Mar 2007

**HAL** is a multi-disciplinary open access archive for the deposit and dissemination of scientific research documents, whether they are published or not. The documents may come from teaching and research institutions in France or abroad, or from public or private research centers.

L'archive ouverte pluridisciplinaire **HAL**, est destinée au dépôt et à la diffusion de documents scientifiques de niveau recherche, publiés ou non, émanant des établissements d'enseignement et de recherche français ou étrangers, des laboratoires publics ou privés.

# **Extinction Coefficients retrieved in Deep Tropical Ice Clouds from Lidar Observations using a CALIPSO-like Algorithm compared to In-Situ Measurements from the Cloud Integrating Nephelometer during CRYSTAL-FACE**

Vincent Noel <sup>1</sup>, D. M. Winker <sup>2</sup>, T. J. Garrett <sup>3</sup>, M. McGill <sup>4</sup>

<sup>1</sup> Laboratoire de Météorologie Dynamique, Palaiseau, France

<sup>2</sup> NASA Langley Research Center, VA, USA

<sup>3</sup> Univ. of Utah, UT, USA

<sup>4</sup> NASA Goddard Space Flight Center, Greenbelt, MD, USA

Submitted to *Atmospheric Chemistry and Physics*

Corresponding author:

Vincent Noel

Laboratoire de Météorologie Dynamique / IPSL

Ecole Polytechnique

91128 Palaiseau, France

[vincent.noel@lmd.polytechnique.fr](mailto:vincent.noel@lmd.polytechnique.fr)

## Abstract

This paper presents a comparison of lidar ratios and volume extinction coefficients in tropical ice clouds, retrieved using observations from two instruments: the 532-nm *Cloud Physics Lidar* (CPL), and the in-situ *Cloud Integrating Nephelometer* (CIN) probe. Both instruments were mounted on airborne platforms during the CRYSTAL-FACE campaign and took measurements up to 17 km. Coincident observations from two cases of ice clouds located on top of deep convective systems are compared. First, lidar ratios are retrieved from CPL observations of attenuated backscatter, using a retrieval algorithm for opaque cloud similar to one used in the recently launched CALIPSO mission, and compared to results from the regular CPL algorithm. These lidar ratios are used to retrieve extinction coefficient profiles, which are compared to actual observations from the CIN in-situ probe, putting the emphasis on their vertical variability. When observations coincide, retrievals from both instruments are very similar, in the limits of colocation. Differences are generally variations around the average profiles, and general trends on larger spatial scales are well reproduced. The two instruments agree well, with an average difference of less than 11% on optical depth retrievals. Results suggest the CALIPSO Deep Convection algorithm can be trusted to deliver realistic estimates of the lidar ratio, leading to good retrievals of extinction coefficients.

# 1. Introduction

Cirrus clouds are high altitude clouds mostly composed of ice crystals. Since they consistently cover more than 30% of the earth's surface (Wylie et al., 1994), their influence on the radiation budget cannot be overlooked (Stephens et al., 1990). The radiative influence of a given cirrus cloud depends mostly on the delicate balance between its albedo and greenhouse effects, and, on a local scale, on its microphysical and optical properties. Most noticeably, the quantity of sunlight reflected by a cirrus cloud (and thus its albedo effect) is directly tied to its

optical thickness  $\tau$ , defined as  $\tau = \int_{z_0}^{z_1} \alpha(z) dz$ : the vertical integration of its extinction coefficient  $\alpha(z)$  between the cloud boundaries  $z_0$  and  $z_1$ . The albedo of a cloud is thus directly dependent on its vertical profile of extinction coefficient. A good knowledge of extinction coefficients, and thus optical depth, in cirrus clouds would lead to a better estimation of their general albedo effect.

Due to the high altitude of cirrus clouds, direct *in situ* measurement of their microphysical properties is a difficult task that cannot be pursued on a systematic basis. Moreover, in the tropics ice clouds are often located on top of deep convective systems (see e.g. Garrett et al. 2004), which means high-altitude observations are a necessity. Because of their large horizontal and vertical extensions, these systems have a large-scale radiative impact on the planet surface and atmosphere (Hartmann et al., 1992), and their creation through fast convection leads to specific microphysic and optical properties (McFarquhar and Heymsfield, 1996; Heymsfield and McFarquhar, 1996). Unfortunately, when conducting satellite studies using passive remote sensing it is often difficult to separate an optically thin ice cloud layer from an underlying convective system, meaning high uncertainties in the retrievals (Chiriaco et al. 2004). This stresses the need for active remote sensing, such as lidar, whose sensitivity

to optically thin clouds makes it one of the most appropriate instruments for cirrus study (Platt, 1973) and can give valuable insights into ice cloud microphysics (Noel et al. 2004). Lidar retrievals of extinction coefficients are an effective tool for studying the optical depth of ice clouds out of reach of in-situ observations, and are not subject to passive remote sensing limitations, as the variability of extinction coefficients is observed as a function of penetration inside the cloud layer. Moreover, the 532-nm spaceborne lidar in the framework of the CALIPSO mission (Winker et al. 2003) is currently producing retrievals of extinction coefficients and thus optical depths on a global scale, even for tropical ice clouds on top of optically thick convective systems.

In the present study, attenuated backscatter profiles observed in deep tropical ice clouds using the *Cloud Physics Lidar* (CPL) on July 28<sup>th</sup> and 29<sup>th</sup> during the *Cirrus Regional Study of Tropical Anvils and Cirrus Layers – Florida Area Cirrus Experiment* (CRYSTAL-FACE, Jensen et al. 2004) are used to retrieve lidar ratios, using the CALIPSO “Deep Convection” retrieval algorithm (Winker, 2003). Results are compared to retrievals using the regular CPL algorithm, then with actual in-situ observations from the airborne collocated probe *Cloud Integrating Nephelometer* (CIN, Garrett et al., 2003). The CRYSTAL-FACE campaign is presented in Sect. 2, along with the instruments used by the present study. The CALIPSO Deep Convection retrieval algorithm is presented and its results compared with results from the CPL algorithm in Sect. 3. Lidar ratio retrievals are then used to retrieve extinction coefficient profiles in Sect. 4, which are compared to in-situ CIN observations. Discussion and conclusion are given in Sect. 5.

## 2. Volume extinction coefficient retrievals during CRYSTAL-FACE

The CRYSTAL-FACE campaign was held in July 2002 over Florida and the Gulf of Mexico, and aimed to provide the comprehensive measurements needed to better understand the microphysical and radiative properties and formation processes of ice clouds on top of thick convective cloud systems. Five mid- to high-altitude aircraft carried numerous *in situ* and remote sensing instruments, with simultaneous ground-based observations. Among these, the NASA *Cloud Physics Lidar* CPL, a three-wavelength (355 nm, 532 nm and 1064 nm) backscatter lidar (McGill et al., 2002), was looking downward from the NASA ER-2 aircraft (King and al. 2003) and provided several days of observations from as high as 20 km, with a vertical resolution of 30 m and an horizontal resolution of 200 m at the typical ER-2 flying speed of 200 m.s<sup>-1</sup>. The CPL telescope field of view is 10~0 μradians, so the footprint on a cloud located less than 10 km away (the typical distance during CRYSTAL-FACE) would be less than 1 meter wide, i.e. roughly 100 times smaller than CALIPSO's. This configuration allowed unique monitoring of ice clouds located on top of tropical convective systems, which would be impossible from the ground because of the lower layers of thick water clouds blocking the lidar penetration. From the raw backscattered laser light measured by the CPL telescope, properties of cloud and aerosol layers are retrieved, including the altitude of cloud base and cloud top, its optical depth  $\tau$ , and profiles of depolarization ratio and volume extinction coefficient. The method used for analysis and retrieval of the volume extinction is explained in McGill et al. (2003), and is based on the standard lidar inversion technique (e.g. Spinhirne et al., 1980; Klett, 1981). When possible (i.e. for optically thin clouds), the lidar

extinction-to-backscatter ratio  $S$  (Sect 3.1) is retrieved directly from lidar observations (through a transmission-loss technique). When this is not possible (i.e. for optically thick clouds such as convective systems),  $S$  is provided below  $-13^{\circ}\text{C}$  by a quadratic function of temperature:  $S = aT^2 + bT + c$  with  $a = -1.42739\text{e-}3$ ,  $b = -2.08944\text{e-}1$  and  $c = 1.5339\text{e+}1$  (Hlavka, private communication, 2005) at a wavelength of 532 nm (a different quadratic function is used at 1064 nm). For temperatures warmer than  $-13^{\circ}\text{C}$ , the value  $S = 17.84$  is used. A very similar technique is used when analyzing observations from the spaceborne *Geoscience Laser Altimeter System* (Zwally et al, 2002).

The CIN probe was mounted on the WB-57 aircraft, which was able to fly through the top of tall convective systems thanks to its high ceiling (up to 18 km). The CIN measures extinction coefficients from the scattering of cloud particles of a 635 nm laser light into sensors, consisting of circular light-diffusing disks and photomultipliers (Gerber et al., 2000). These sensors measure the forward-scattered and backscattered light between  $10^{\circ}$  and  $175^{\circ}$ , from which the volume extinction parameter is inferred based on an estimate of the light forward-scattered by diffraction (Eq. 7 in Gerber et al., 2000). Since diffraction is necessarily one half of scattered energy, the omitted fraction is constrained and is estimated to be  $0.57 \pm 0.02$ . The lower threshold for extinction measurement by the CIN was  $0.0004 \text{ m}^{-1}$  and the estimated uncertainty in the measurements during CRYSTAL-FACE was 15% for values of extinction greater than about  $0.001 \text{ m}^{-1}$ . This error estimate has since been validated using ground and airborne transmissometer probes (Gerber, 2007; Garrett, 2007), which are less sensitive than the CIN but are entirely first principles.

### 3. The CALIPSO Deep Convection Algorithm

#### 1. Lidar ratio retrieval

For elastic backscatter lidars, volume extinction coefficient profiles  $\alpha(z)$  are retrieved from observations of attenuated backscatter profiles  $\beta(z)$ . In order to do so, a relationship between the backscatter and extinction coefficients must be assumed. Often defined as  $S = \frac{\alpha}{\beta}$ , the lidar ratio, this relation is assumed to stay constant within a cloud layer.

The magnitude of the lidar ratio depends on the microphysical properties of the cloud, but in many cases can be retrieved from attenuated backscatter observations alone. In the routine analysis of CALIPSO observations, different algorithms are used depending on the opacity of the atmospheric layer. For semi-transparent clouds, a transmittance algorithm is used, based on the difference in lidar return signal from clear regions above and below the cloud layer. In the case of fully attenuating layers, such as deep tropical thick convective systems, the transmittance algorithm cannot be applied, as the laser cannot penetrate the full layer and no signal is available beyond the cloud layer. An equation can be derived which relates the cloud-integrated attenuated backscatter signal  $\gamma'$  to the cloud transmittance  $T$  (Platt 1973; Platt et al 1999):

$$\gamma' = \frac{1 - T^2}{2S\eta} \quad (1)$$

where  $\eta$  is a multiple scattering correction factor. In the case of an opaque cloud layer,  $T = 0$  so that  $\gamma' = \frac{1}{2S\eta}$ . The lidar ratio can thus be retrieved from lidar profiles of attenuated backscatter and an estimate of  $\eta$ . This is the essence of the algorithm used by CALIPSO to retrieve extinction in the tops of deep convective clouds (Winker, 2003). This algorithm



assumes that a mean lidar ratio can be used for an entire lidar profiles, hence it supposes an homogeneous microphysical composition throughout the cloud layer ; since the lidar penetration is limited in optically thick convective systems this is a reasonable assumption.

## ***2. Lidar ratio retrieval on July 29<sup>th</sup>***

On July 29<sup>th</sup>, a CRYSTAL-FACE mission focused on a small-scale convective system (McGill et al. 2004) that extended horizontally over 100 km and up to the tropopause (higher than 14 km), meaning the highest several kilometers were composed of ice crystals. CPL observations of attenuated backscatter between 19:18 and 19:42 are shown in Fig. 1 as a function of time and altitude, on a logarithmic color scale. During this timeframe, the ER-2 carrying the CPL flew over the convective system in a straight line, and CPL observations show the top of the system rises from 12 km at its edges to more than 14 km in its central area, close to the convective center. The CPL was able to penetrate the cloud layer at least one kilometer before the laser signal was completely attenuated (Fig. 1), but coincident observations from the *Cloud Radar System* (not shown, Li et al, 2004), also mounted on the ER-2, show this cloud system extended down to the surface.

The lidar ratios retrieved during the same timeframe are shown in Fig. 2, using the CPL algorithm (in black) and the CALIPSO Deep Convection algorithm described above (in red). Because of the small field of view of the CPL instrument and the nearness of the cloud, multiple scattering is insignificant, and the lidar ratio equation (Eq. 1) can be simplified  $S=1/2\gamma'$ . It should be noted that it will only be possible to extrapolate conclusions from the current study to CALIPSO retrievals as far as a valid multiple scattering correction factor is available when using the full Eq. 1 during the CALIPSO analysis. The two sets of values are very similar, most in the 20-40 range, with some outlier points up to 80. In the opaque portions of the cloud, the agreement is very good; near the cloud edges (not opaque), values

derived using the Deep Convection algorithm are too large. In this case, the CALIPSO operational code uses a more appropriate transmittance-based retrieval.

The same comparison was conducted on all cloud layers detected on July 29<sup>th</sup>, and on similar observations made on July 28<sup>th</sup>. The average difference and its standard deviation are shown on a logarithmic scale in Fig. 3, as a function of the minimum considered optical depth  $\tau_{min}$ . When considering all cloud layers ( $\tau_{min} = 0$ ), the average difference goes as high as 100 for July 28<sup>th</sup>, showing the Deep Convection algorithm leads to unrealistic results in such conditions, as expected. However, as  $\tau_{min}$  increases, the difference quickly decreases below 10 for  $\tau_{min} = 0.3$  (July 29<sup>th</sup>) and  $\tau_{min} = 1$  (July 28<sup>th</sup>), down to 2 (July 29<sup>th</sup>) and 1 (July 28<sup>th</sup>) for  $\tau_{min} > 2$ . The standard deviation simultaneously goes through the same decrease, dropping from values greater than 100 to less than 5. The decrease is especially important for July 28<sup>th</sup>. Fig. 3 shows that the CALIPSO Deep Convection algorithm is well suited to the study of optically thick cloud layers.

### 3. Extinction retrieval

Using the CPL attenuated backscatter observations (Sect. 3.1) and the retrieved lidar ratios (Sect. 3.2), it is possible to retrieve the actual particulate backscatter  $\beta(z)$  at the altitude  $z$  from the well-known forward solution to the lidar equation (Platt et al, 1973):

$$\beta(z) = \frac{\beta'(z)}{1 - 2\eta S \int \beta'(z') dz'} \quad (2)$$

with  $\beta'(z)$  the observed attenuated backscatter, and  $z_0$  the altitude of lidar penetration in the layer (i.e. the cloud top for a nadir-looking lidar like the CPL). As the goal of this study is an operational validation of the CALIPSO Deep Convection algorithm (Sect. 3.1), a simple application of this algorithm will provide a good first approximation for comparison purposes.

Once backscatter profiles  $\beta(z)$  are retrieved, extinction coefficients  $\alpha(z) = \beta(z) \cdot S(z)$  can be easily obtained for any given layer (Sect. 3.1). This technique was applied to CPL observations of attenuated backscatter in ice clouds from July 28<sup>th</sup> and 29<sup>th</sup> (Sect. 3.2). Results of these retrievals will be presented and compared to in-situ probe observations in the next section.

## 4. Coincident observations of extinction in cirrus clouds

During CRYSTAL-FACE, cirrus clouds were observed many hours by the CPL (on the ER-2) and the CIN (on the WB-57), but most of the time the observations were not simultaneous. This part of the study will focus on the periods of time when the two instruments were functioning simultaneously and their two aircraft were flying in the same area, so that the two instruments were monitoring the same cloud. To evaluate the variability of extinction with altitude, and the correlation between results from both instruments, only cases when the WB-57 was either climbing or descending in the cloud layer were considered. Periods of observation fitting this description for July 28<sup>th</sup> and 29<sup>th</sup> are described in Table 1. For each CPL profile, coordinates of the supporting ER-2 aircraft were compared to those of the WB-57 in the timeframe of coincidence, the maximum delay between both aircraft being 10 minutes.

As seen in Sect. 3.2, the July 28<sup>th</sup> and 29<sup>th</sup> cases are typical of the small-scale convective systems that developed frequently in the tropical area monitored during CRYSTAL-FACE. Volume extinction coefficients retrieved from CPL backscatter observations using the CALIPSO Deep Convection algorithm (Sect. 3.1 and 3.3) are shown in Fig. 4 (July 28<sup>th</sup>) and Fig. 5 (July 29<sup>th</sup>), with the WB-57 altitude at coincident points plotted over in red symbols. On July 28<sup>th</sup>, the lidar penetration depth is very variable on time scales of less than a minute:

most profiles are fully attenuated before the signal reaches 13 km; however some isolated profiles show deeper penetration and reach 13 km (e.g. around 22:57). This seems due to rapid small-scale variations in the spatial distribution of cloud water content. The extinction coefficient is generally in the  $10^{-3}$  to  $3 \cdot 10^{-3} \text{ m}^{-1}$  range (green on the color scale). The studied timeframe on July 29<sup>th</sup> (Fig. 5) shows a stable lidar penetration depth, 1 km on average, but is less homogeneous, with wider variations in retrieved extinction values (from  $5 \times 10^{-4}$  to  $10^{-2} \text{ m}^{-1}$ ). Integrating these extinction profiles gives a highly variable time series of optical depths (not shown), with values typically ranging between 1 and 4. As the optical depth approaches these higher values, the retrievals become unreliable for two reasons: 1) it is well known that the forward solution becomes unstable at high optical depths and can become divergent (Platt et al., 1987), and 2) the backscatter return signal becomes very weak and noise excursions influence the retrieved values. Thus extinction coefficients at low altitudes, such as the very high extinctions at the largest penetration depths (red on the color scale in Fig. 4 and 5) should be treated with caution.

For each CPL profile, extinction coefficients were extracted from the CIN data at the point of closest WB-57 and ER-2 coincidence. On July 28<sup>th</sup>, the WB-57 went from 13 km at 22:45 up to 16 km around 23:00 (Fig. 4), a cloud was observed between 22:45 and 22:50 ; the ER-2 flew over the same area between 22:55 and 23:00. To sample the maximum of cloud data, the WB-57 was often spiraling inside cloud systems, which is why these points are not in chronological order. The extinction observed by the CIN during this period is shown as symbols in Fig. 6 as a function of altitude, with horizontal bars showing the uncertainty. The average extinction profile retrieved from CPL observations during the same timeframe is shown in full line, the shaded area showing the standard deviation around the average. The agreement between both instruments is good between 13.7 and 15 km, with an average

difference of  $0.166 \times 10^{-2} \text{ m}^{-1}$  between profiles, which implies that the Deep Convection algorithm is choosing appropriate values for  $S$ . Below 13.7 km, collocation between aircraft was not sufficient for comparison. The lidar sees large values of extinction (up to  $10^{-2} \text{ m}^{-1}$ ) down to 13.0 km where the signal gets totally attenuated (radar data shows the cloud base was actually much lower). For colocated measurements, the time difference and horizontal distance between aircraft are not correlated with difference in extinction coefficients. Integrating both CPL and CIN profiles of extinction coefficient over the correlated regions (13.7 to 15 km) leads to respective optical depths  $\tau$  of 1.87 and 1.67 (Table 2), i.e. the CPL-derived value is 11% larger than the CIN-derived value, within the measurement uncertainties of the two instruments. This difference is negligible in radiative terms, given the limited penetration of the CPL. Integrating the CPL extinction profile over the full layer (i.e. 13 to 15 km) gives a much higher value of  $\tau = 4.6$ . This is a very high optical depth for a lidar to penetrate, and indicates the variability of the profile below about 13.7 km may be due to weak signal and the lowest part of the profile is probably unreliable. The CIN detects some low extinction coefficients ( $\alpha < 5 \times 10^{-4} \text{ m}^{-1}$ ) at the tropopause level (15.5 km according to radiosoundings launched at 23:00 from Tampa, 27.70N, 82.40W) that do not appear in the lidar retrievals (Fig. 6); these values are very close to the CIN noise level ( $4 \times 10^{-4} \text{ m}^{-1}$ ) and should not be considered as actual particles.

On July 29<sup>th</sup>, the WB-57 went from 12.5 km at 20:00 up to 14 km at 20:04, then down again at 20:12 (red symbols in Fig. 5). CIN observations of extinction, averaged over altitude bins during this period (Fig. 7) are similar to CPL retrievals using the CALIPSO Deep Convection algorithm (the large error bars in CIN extinctions are due to the existence of several data points in a single altitude bin). Consistent with Fig. 5, high extinction coefficients (larger than  $5 \cdot 10^{-3} \text{ m}^{-1}$ ) are observed. Both profiles are in good agreement from cloud top (14 km) down to

12.5 km, where the colocation between aircraft is too low. The simultaneous sudden break in lidar observations at 12.5 km is due to total signal attenuation, as radar observations show a lower cloud base. As in the July 28<sup>th</sup> case, CPL retrievals are highly variable at low altitudes (e.g. below 13 km), due to weak signal and the limited stability of the inversion algorithm. Integration of extinction profiles leads to very high optical depths (Table 2): 4.74 and 5.08, respectively for the CPL and the CIN. These values are consistent with the full-profile optical depth for July 28<sup>th</sup> (4.6). The slightly lower optical depth from CPL extinctions is consistent with total lidar signal attenuation.

## 5. Discussion and conclusion

This study presents a comparison between volume extinction coefficients observed from a CIN in-situ probe and retrievals from lidar backscattering profiles (Sect. 2). Three coincident observation periods are compared, highlighting the variability with altitude (Sect. 4). Results show a very good agreement between both instruments, for extinction coefficients sometimes as low as  $10^{-3} \text{ m}^{-1}$  (Fig. 2). This implies the CALIPSO Deep Convection algorithm is doing a good job at selecting lidar ratios for opaque clouds. However, this conclusion was reached using using CPL observations where multiple scattering effects are negligible. Since the footprint of actual CALIPSO observations will be roughly 100 times wider than with CPL, multiple scattering effects will have to be accounted for using an appropriate multiple scattering correction factor (Eq. 1). Retrieval of this parameter depends on additional algorithms and observations and hence is outside the scope of the validation of the Deep Convection algorithm itself.

Overall the extinction coefficient profiles retrieved from CPL observations show higher small-scale variability (in the 100-meters range) than the CIN observations, mostly due to the

fact that CIN observations were averaged over 11 seconds periods in order to increase the signal-to-noise ratio. The CPL variability can be explained by the unstable nature of the extinction retrieval algorithm (Eq. 2) at high optical depths, which creates large fluctuations in backscattering coefficient from one profile to the next – small-scale variations in CPL retrievals should therefore be treated with caution, as they may not be physical. Overall, CIN observations are often contained within the standard deviation of CPL retrievals. As variations on larger scales are well reproduced, the retrieved optical depth is only slightly affected (6 and 11% difference between the two instruments when considering intersecting observations). In the second case (July 29<sup>th</sup>), the extinction coefficients retrieved from the lidar were slightly lower than those observed in-situ by the CIN. This can be explained by the lidar signal being fully attenuated by the optically thick layer of the convective systems, and thus unable to penetrate the whole cloud layer measured by the CIN. Overall, the lidar performs reasonably well in such extreme conditions (i.e. very thick convective system), and as it was shown previously those differences are only significant on small spatial scales and are only a secondary influence on larger scale trends and integrated results.

Differences in extinction coefficients still exist, though, and might be due to instrumental and algorithmic limitations in both retrieval schemes or spatial and temporal mismatch. For instance, the lidar ratio is assumed to stay constant in all cloud profiles (Sect. 3.1), which is unrealistic if large changes in microphysical properties happen on a single profile basis. A study of ice crystal shape classification from depolarization ratios suggests only limited change in microphysics with altitude above 12 km in convective cases observed on July 28 and 29 during CRYSTAL-FACE (Noel et al. 2004b), however small-scale variations are still possible. Regarding the CIN, as with many other probes, it has been argued that ice crystals can shatter when impacted by the aircraft or the probe itself, leading to an artificial increase in

small particles concentration. Recent comparisons between collocated in-situ probes during CRYSTAL-FACE (Heymsfield et al, 2006) suggest that due to this phenomenon, observations from the CIN might overestimate the extinction coefficient, potentially by as much as a factor of 2. Gerber (2007) and Garrett (2007) have rebutted this work, arguing that the inferred errors were the result of faulty or inappropriate comparisons. Nonetheless, additional work might therefore be required to determine if the good agreement found between results from both instruments in the present study is the byproduct of distinct observational and analysis biases in each instrument, which would compensate for each other and coincidentally lead to similar results. On the other hand, the fact that results from both instruments, using very different techniques, show a good agreement strengthens the confidence in extinction coefficients retrieved from both instruments. Moreover, even in the case of a quantitative bias, the fact that the variations of extinction coefficient are similar with altitude in same-day profiles from each instrument still suggests the vertical variability of lidar retrievals can be trusted. In any case, retrievals from both instruments are consistent for low values of extinction (below  $10^{-3} \text{ m}^{-1}$ ) that would still remain small after a numerical correction. The results are especially important since retrievals from the spaceborne CALIPSO mission (Winker et al. 2003) will soon be available, leading to an extensive mapping of ice cloud optical and microphysical properties.

## **ACKNOWLEDGMENTS**

*This research was supported in part by the NASA Langley Research Center under contract NAS1-02058. The Cloud Physics Lidar is sponsored by NASA's Radiation Sciences Program and by NASA's Earth Observing System (EOS) office.*



## References

- Chiriaco M., H. Chepfer, V. Noel, A. Delaval, M. Haeffelin, P. Dubuisson and P. Yang, 2004: Improving Retrievals of Cirrus Cloud Particle Size Coupling Lidar and Three-channel Radiometric techniques, *Monthly Weather Review* **132**, 1684-1700
- Garrett T. J., H. Gerber, D. G. Baumgardner, C. H. Twohy, D. G. Baumgardner, and E. M. Weinstock, 2003: Small, highly reflective ice crystals in low-latitude cirrus. *Geophys. Res. Lett.* **30**, doi:10.1029/2003GL018153.
- Garrett T. J., A. J. Heymsfield, M. J. McGill, B. A. Ridley, D. G. Baumgardner, T. P. Bui and C. R. Webster 2004 : Convective generation of cirrus near the tropopause *J. Geophys. Res.* **109**, D21203
- Garrett T. J. 2007: Comment on “Effective radius of ice cloud particle populations derived from aircraft probes” by Heymsfield et al. (2006). *J. Atmos. Ocean. Tech.*, accepted.
- Gerber H., Y. Takano, T. J. Garrett and P. V. Hobbs 2000: Nephelometer measurements of the Asymmetry parameter, Volume extinction coefficient and Backscatter ratio in Arctic clouds, *J. of Atmos. Sci.* **57**, 3021-3034
- Gerber et al. 2007: Comment on “Effective radius of ice cloud particle populations derived from aircraft probes” by Heymsfield et al. (2006). *J. Atmos. Ocean. Tech.*, accepted.
- Hartmann, D. L. and Ockert-Bell, M. E. and Michelsen, M. L. 1992: The effect of cloud type on earth's energy balance : Global analysis, *J. of Climate* **5** , 1281-1304
- Heymsfield, A. J. and McFarquhar, G. M. 1996: On the high albedos of anvil cirrus in the tropical pacific warm pool: microphysical interpretations from CEPEX and from

Kwajalein, Marshall Islands, *J. Of Atmos. Sci.* **53** , 2401-2423

- Heymsfield A. J., C. Schmitt, A. Bansemer, G.-J. Van Zadelhoff, M. J. McGill, C. Twohy, D. Baumgardner, 2006: Effective Radius of Ice Cloud Particle Populations Derived from Aircraft Probes. *J. Atmos. Ocean. Technol.* **23** 361-380.
- Hlavka, D. L., 2005: Private communication.
- Jensen E. J., D. Starr and O. B. Toon 2004: Mission investigates tropical cirrus clouds. *EOS* **85**, 45-50.
- King, M. D., S. Platnick, C. C. Moeller, H. E. Revercomb, and D. A. Chu, 2003: Remote sensing of smoke, land, and clouds from the NASA ER-2 during SAFARI 2000, *J. Geophys. Res.* **108**(D13), 8502, doi:10.1029/2002JD003207.
- Klett J. D., 1981: Stable analytical inversion solution for processing lidar returns. *Applied Optics* **20**, 211-220.
- Li L., G. M. Heymsfield, P. E. Racette, L. Tian and E. Zenker, 2004: A 94-GHz cloud radar system on a NASA high-altitude ER-2 aircraft, *J. Atmos. Oceanic. Technol.* **21** (9), 1378-1388.
- McFarquhar, G.M. and Heymsfield, A. J. 1996: Microphysical characteristics of three cirrus anvils sampled during the Central Equatorial Pacific Experiment (CEPEX), *J. Of Atmos. Sci.* **52**, 2401-2423
- McGill M. J., D. L. Hlavka, W. D. Hart, J. D. Spinhirne, V. S. Scott and B. Schmid 2002: The Cloud Physics Lidar: Instrument description and initial measurement results. *Applied Optics* **41**, 3725-3734
- McGill M. J., D. L. Hlavka, W. D. Hart, E. J. Welton and J. R. Campbell 2003: Airborne lidar measurements of aerosol optical properties during SAFARI 2000. *J. Of Geophys. Res.* **108**, 8493.

- McGill, M. J., L. Li, W. D. Hart, G. M. Heymsfield, D. L. Hlavka, P. E. Racette, L. Tian, M. A. Vaughan, and D. M. Winker, 2004: Combined lidar-radar remote sensing: Initial results from CRYSTAL-FACE *J. Geophys. Res.* **109**, D07203.
- Noel V., H. Chepfer 2004: Study of ice crystal orientation in cirrus clouds based on satellite polarized radiance measurements. *J. Of Atmos. Sci.* **61**, 2073-2081
- Noel V., D. Winker, M. McGill and P. Lawson, 2004: Classification of particle shapes from lidar depolarization ratio in convective ice clouds compared to in situ observations during CRYSTAL-FACE. *J. Of Geophys. Res.* **109**, D24213
- Platt, C.M.R. 1973: Lidar and Radiometric observations of cirrus clouds, *J. Of Atmos. Sci.* **30**, 1191-1204
- Platt C.M.R., J. C. Scott and A. C. Dilley 1987: Remote sensing of high clouds. Part VI: Optical properties of midlatitude and tropical cirrus. *J. Atmos. Sci.* **44** (4), 729-747.
- Platt C. M. R., D. M. Winker, M. A. Vaughan and S. D. Miller, 1999: Backscatter-to-extinction in the Top Layers of Tropical Mesoscale Convective Systems and in Isolated Cirrus from LITE observations. *J. Appl. Met.* **38**, 1330-1345.
- Spinhirne J. D., J. A. Reagan and B. M. Herman 1980: Vertical Distribution of Aerosol Extinction Cross-Section and Inference of Aerosol Imaginary Index in the Troposphere by Lidar Technique. *J. of App. Met.* **19** (4), 426–438.
- Stephens, G. L. and Tsay, S.-C. and Stackhouse, P. W. and Flatau, P. J. 1990: The relevance of the microphysical and radiative properties of cirrus clouds to climate and climate feedback *J. Of Atmos. Sci.* **47**, 1742-1753
- Winker, D. M. and Pelon, J. and McCormick, M. P. 2003: The CALIPSO mission: Spaceborne lidar for observation of aerosols and clouds. *Proc. SPIE*, 4893, 1-11

- Winker D. M., 2003: Accounting for Multiple Scattering in Retrievals from Space Lidar, *Proc. SPIE* 5059, 128-139.
- Wylie, D. P. and Menzel, W. P. and Woolf, H. M. and Strabala, K. L. 1994: Four Years of Global Cirrus clouds statistics using HIRS, *J. Of Climate* 7 , 315-335
- Zwally, H.J., B. Schutz, W. Abdalati, J. Abshire, C. Bentley, A. Brenner, J. Bufton, J. Dezio, D. Hancock, D. Harding, T. Herring, B. Minster, K. Quinn, S. Palm, J. Spinhirne, and R. Tomas, 2002: ICESat's Laser Measurements of Polar Ice, Atmosphere, Ocean, and Land. *J. Of Geodyn.* **34**, 405-445.

## Table captions

Table 1. Properties of each case of collocated observations from the CPL and CIN during CRYSTAL-FACE.

Table 2. Cloud optical depth  $\tau$  obtained from integration of volume coefficient profiles from the CPL and CIN observations.

	July 28 <sup>th</sup>	July 29 <sup>th</sup>
Time of observation	22:45 – 23:00	20:01 – 20:12
WB-57 Altitude range	13.5 – 16 km	12.5 – 14 km

Table 1. Properties of each case of collocated observations from the CPL and CIN during CRYSTAL-FACE.

	<i>July 28<sup>th</sup></i>	<i>July 29<sup>th</sup></i>
From CPL observations	1.87	5.08
From CIN observations	1.67	4.74

Table 2 : Cloud optical depths  $\tau$  obtained from integration of volume coefficient profiles from the CPL and CIN observations.

## 6. Figure Captions

Fig. 1: Attenuated backscatter observed by the CPL as a function of time and altitude from 19:18 to 19:42 on July 29<sup>th</sup> 2002, using a logarithmic color scale (arbitrary units).

Fig 2: Lidar ratios  $S$  for the same time period shown in Fig. 1, using the CPL retrieval algorithm (black) and the CALIPSO Deep Convection algorithm (red).

Fig 3: Difference between lidar ratio  $S$  values retrieved using the CALIPSO Deep Convection algorithm and the CPL retrieval algorithm: average (left), standard deviation (right) as a function of the minimum considered optical depth.

Fig. 4: Extinction ( $\text{m}^{-1}$ ) retrieved from CPL backscatter observations and lidar ratio from the CALIPSO algorithm, between 22:55 and 23:00 on July 28<sup>th</sup> 2002, using a logarithmic color scale. The path of the WB-57, carrying the CIN probe, is plotted in red.

Fig. 5: Same as Fig. 4, for July 29<sup>th</sup> 2002 between 19:45 and 19:59.

Fig. 6: Profile of extinction coefficients ( $\text{m}^{-1}$ ) retrieved from CPL observations using the CALIPSO Deep Convection algorithm (average profile in full line, standard deviation in shaded grey) and from CIN collocated observations (crosses, with instrument uncertainty shown as horizontal bars) for the July 28<sup>th</sup> case, as a function of altitude (km).

Fig. 7: Same as Fig. 6, for the July 29<sup>th</sup> case.



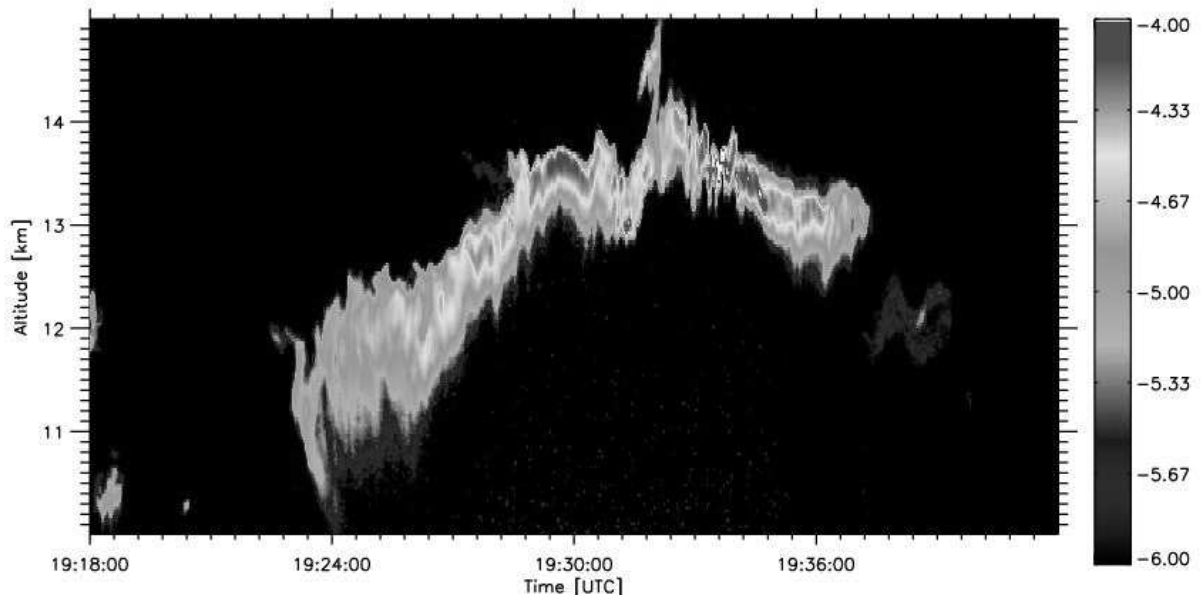


Fig. 1: Attenuated backscatter observed by the CPL as a function of time and altitude, from 19:18 to 19:42 on July 29<sup>th</sup> 2002 using a logarithmic color scale (Arbitrary Units).

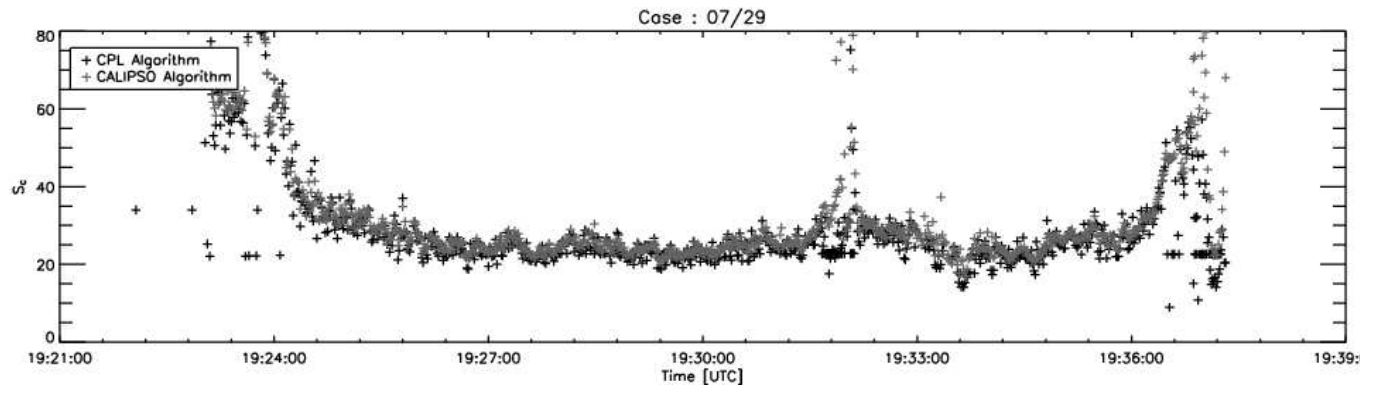


Fig 2: Lidar ratios  $S$  for the same time period shown in Fig. 1, using the CPL retrieval algorithm (black) and the CALIPSO Deep Convection algorithm (red).

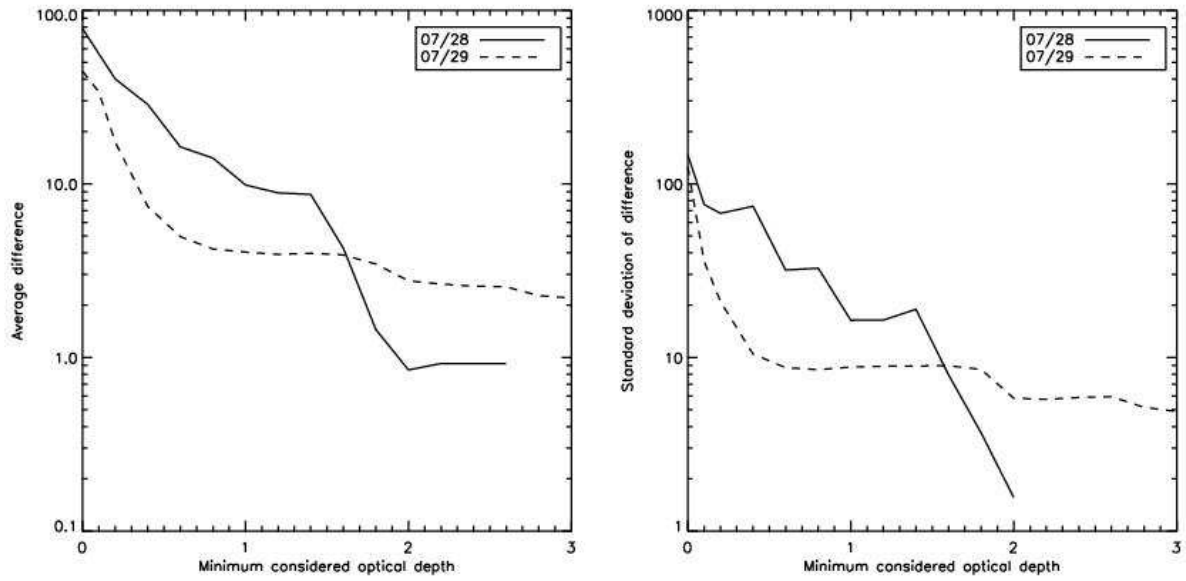


Fig 3: Difference between lidar ratio  $S$  values retrieved using the CALIPSO Deep Convection algorithm and the CPL retrieval algorithm: average (left), standard deviation (right) as a function of the minimum considered optical depth.

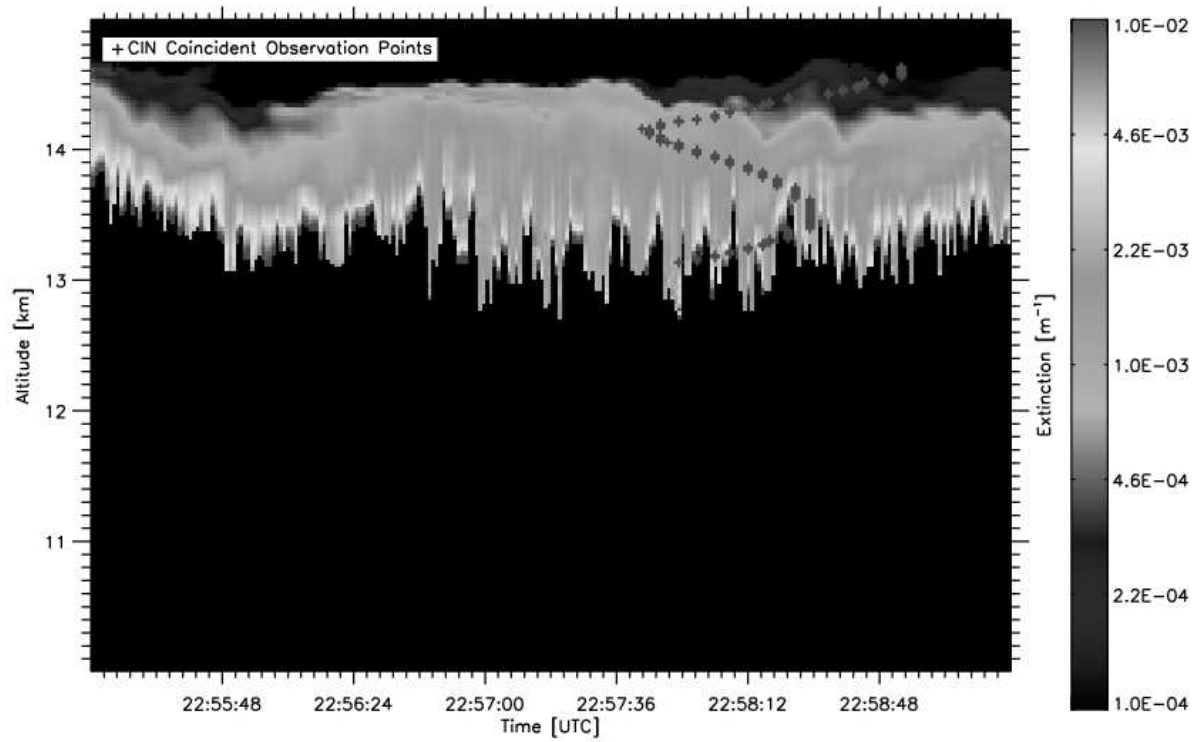


Fig. 4: Extinction ( $\text{m}^{-1}$ ) retrieved from CPL backscatter observations and lidar ratio from the CALIPSO algorithm, between 22:55 and 23:00 on July 28<sup>th</sup> 2002, using a logarithmic color scale. The path of the WB-57, carrying the CIN probe, is plotted in red.

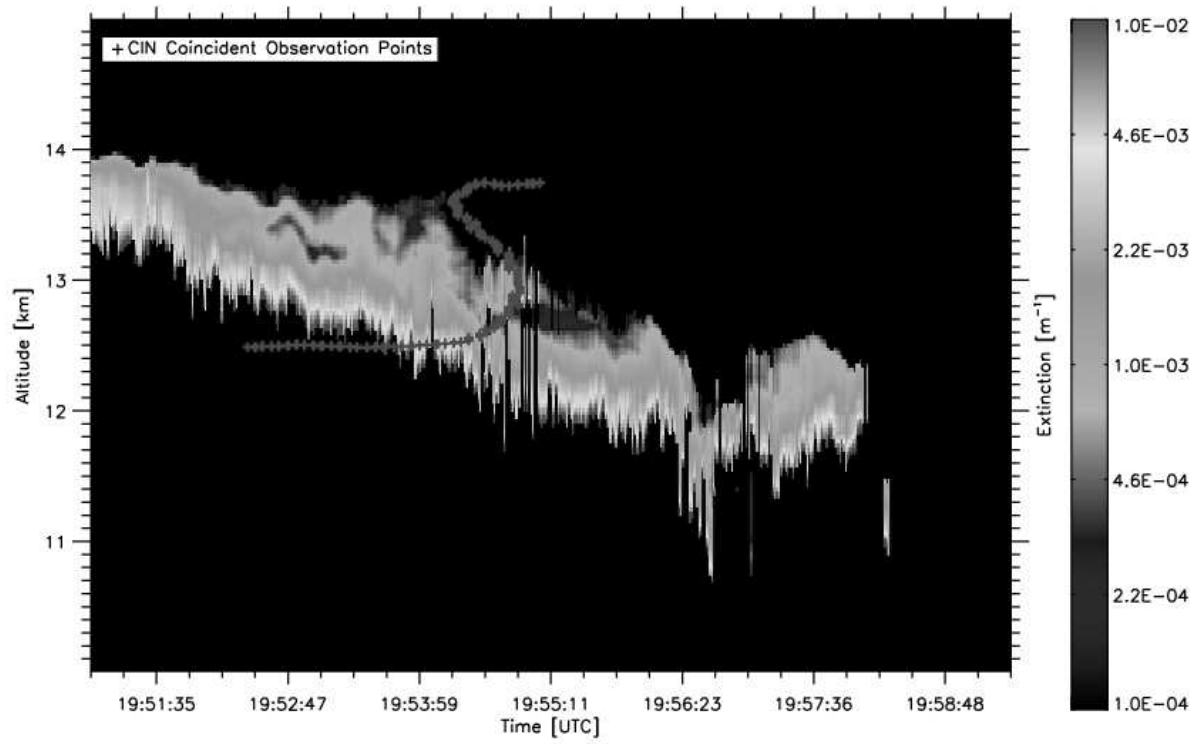


Fig. 5: Same as Fig. 4, for July 29<sup>th</sup> 2002 between 19:45 and 19:59.

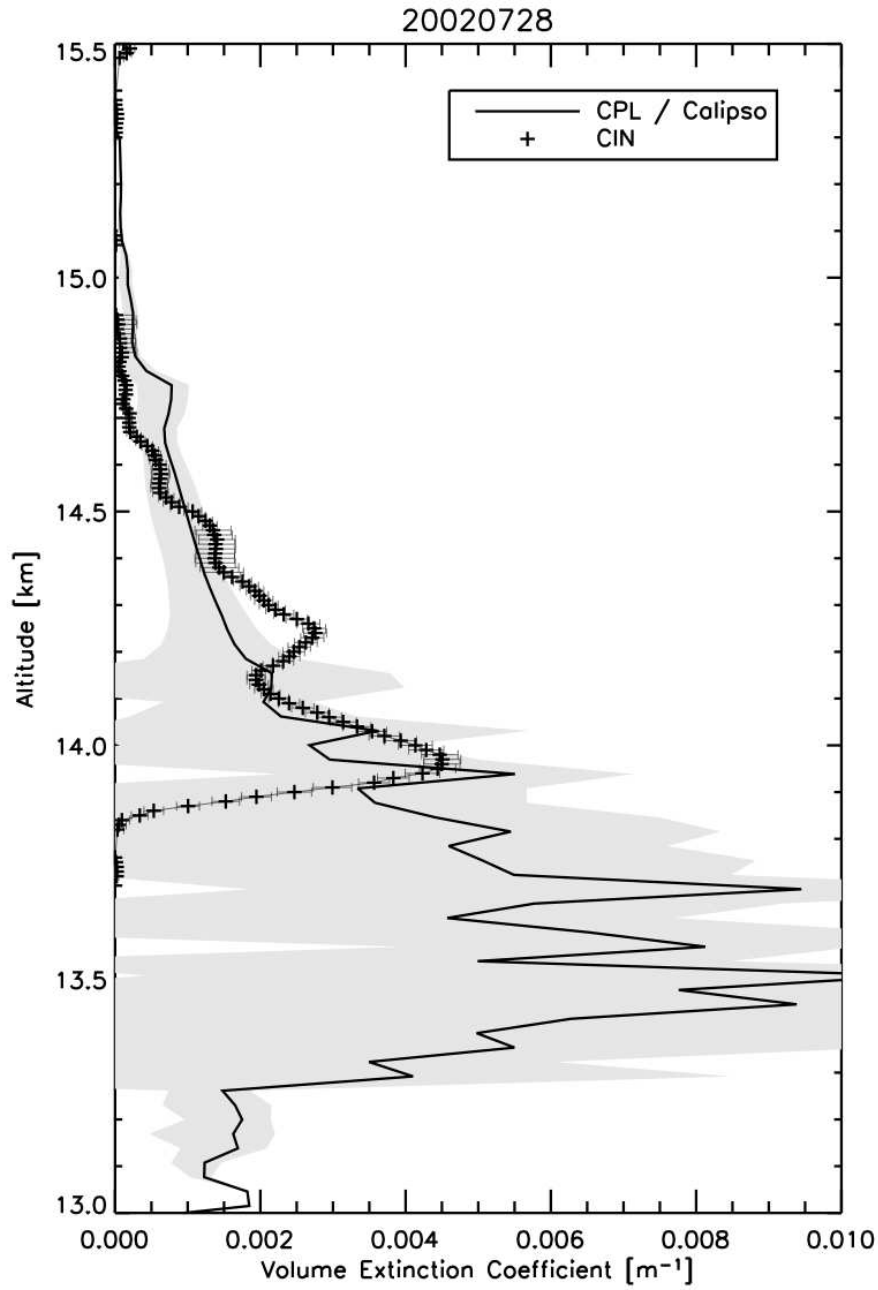


Fig. 6: Profile of extinction coefficients ( $\text{m}^{-1}$ ) retrieved from CPL observations using the CALIPSO Deep Convection algorithm (average profile in full line, standard deviation in shaded grey) and from CIN collocated observations (crosses, with instrument uncertainty shown as horizontal bars) for the July 28<sup>th</sup> case, as a function of altitude (km).

QuickTime™ et un  
décompresseur TIFF (non compressé)  
sont requis pour visionner cette image.

Fig. 7: Same as Fig. 6, for the July 29<sup>th</sup> case.